Intelligent Control for Enhanced Phase-Locked Loop Performance in Grid-Connected Inverters

Noussaiba Mennai[1,*], Ammar Medoued[1], Youcef Soufi[2] and Abdallah Faleh[3]

[1]Dept. electrical engineering, LES Laboratory, University of 20 August 1955, Skikda, Algeria
[2]Dept. electrical engineering, LABGET Laboratory, Larbi Tebessi University, Tebessa, Algeria
[3]Dept. electromechanical, University Mohamed El Bachir El Ibrahimi, Bordj Bou Arreridj, Algeria

Abstract

This research paper focuses on the modeling and design of both conventional proportional-integral (PI) and a proposed intelligent fuzzy logic controller (FLC) applied to synchronous reference frame phase-locked loops (SRF-PLLs), commonly used as synchronization units for grid-connected inverters. Ensuring the optimal performance of this unit is crucial, especially during the injection of current into the grid. To achieve the best PLL performance, the proposed FLC-based SRF-PLL and conventional PI-based SRF-PLL were evaluated within the context of a 1-megawatt (MW) three phase grid-connected voltage source inverter (VSI) current controller predefined model. The simulation results in Matlab/Simulink revealed that the proposed FLC controller significantly improved the performance of the PLL within the system compared to the PI controller.

Keywords

Grid Synchronization, Phase-locked loop (PLL), Grid-connected inverter, Fuzzy logic controller (FLC), PI controller

1. Introduction

The amount of power used worldwide is rising quickly, surpassing the capacity that traditional fossil fuels can accommodate. In response to this challenge, modern environmental rules advise the widespread use of renewable energy sources (RES) in the context of distributed generation (DG) or microgrids (MG) to solve this issue. The integration of RES into the grid is essential; however, it requires careful placement, improved grid-connected inverter control techniques, and synchronization processes to prevent disruptions and instability in the utility grid.

There have been a lot of studies done in the past few years on phase-locked loop (PLL) techniques, which play a critical role in grid-connected power converters to enable precise synchronization of the converter with the grid voltage. M. P. Thakre et *al.* [1] presented an overview of both basic and advanced PLL methods, such as synchronous reference frame PLL (SRF-PLL), also known as dq-PLL, stationary reference frame PLL ($\alpha\beta$-PLL), dual second-order generalized integrator (DSOGI-PLL), etc., under various grid conditions. However, it is noteworthy that all PLLs discussed in the study are equipped with a PI controller, similar to the limitation observed in [2] and [3]. In contrast, authors in [4] applied fuzzy logic to enhance the PLL performance of an induction heating supply system, which is a very narrow application. Also, the modeling is very basic, and the stability analysis is minimal. Similarly, M. Sibanyoni et *al.* [5] did not delve deeper into mathematical modeling when integrating fuzzy logic control into the loop filter of a SOGI-PLL, and their study was limited to a single-phase PV inverter application. On the other hand, researchers in [6] proposed using a Mamdani inference fuzzy controller to replace the PI controller in the loop filter of an SRF-PLL. While novel, the design and tuning process of the fuzzy and PI-based SRF-PLL are covered in less detail. Furthermore, the lack of essential components such as an LCL filter and transformer in the simulation model makes the test system less practical and representative of real three-phase grid-connected inverter systems.

The aim of this paper is to enhance the performance of the grid-connected inverter's synchronization unit, namely the SRF-PLL since it is the most used, by replacing the traditional PI controller with the proposed fuzzy logic controller. For that, both controllers were designed and tuned. Subsequently, simulation results were obtained in the Matlab/Simulink environment by integrating these PLLs into a current controller of a 1 MW three-phase grid-connected voltage source inverter (VSI) and comparing the results.

6th International Hybrid Conference On Informatics And Applied Mathematics, December 6-7, 2023 Guelma, Algeria
*Corresponding author.
n.mennai@univ-skikda.dz (N. Mennai);
a.medoued@univ-skikda.dz (A. Medoued);
youcef.soufi@univ-tebessa.dz (Y. Soufi);
abdallahfalehfr@gmail.com (A. Faleh)
0000-0002-6344-0789 (N. Mennai); 0000-0003-4073-6883 (A. Faleh)

2. PI Based SRF-PLL Modeling and Controller Tuning

2.1. Mathematical Model of SRF-PLL

For balanced three phase grid voltages with a phase θ and peak value V_m shifted from one another by 120 degrees as described in Eq. (1), clark and park transformation in Eqs. (2) and (3) are used to convert the grid voltage V_{abc} to $V_{\alpha\beta}$ in stationary reference frame then to SRF components V_{dq} [7]. By lining up the d-axis voltage V_d with the phase voltage V_a, it is possible to determine the phase angle by maintaing the quadrature component V_q to zero by using the PI controller [8]. With ω_0 is the feed-forward frequency added to create the estimated rotation frequency $\omega^{'}$, which is integrated to get the estimated phase angle $\theta^{'}$ in radians. This process is seen in Fig. 2.

$$\begin{cases} V_a = V_m \sin(\theta) \\ V_b = V_m \sin(\theta - \frac{2\pi}{3}) \\ V_c = V_m \sin(\theta + \frac{2\pi}{3}) \end{cases} \tag{1}$$

$$\begin{bmatrix} V_\alpha \\ V_\beta \end{bmatrix} = \frac{2}{3} \begin{bmatrix} 1 & \frac{-1}{2} & \frac{-1}{2} \\ 0 & \frac{\sqrt{3}}{2} & \frac{-\sqrt{3}}{2} \end{bmatrix} \begin{bmatrix} V_a \\ V_b \\ V_c \end{bmatrix} \tag{2}$$

$$\begin{bmatrix} V_d \\ V_q \end{bmatrix} = \begin{bmatrix} \cos\theta^{'} & \sin\theta^{'} \\ -\sin\theta^{'} & \cos\theta^{'} \end{bmatrix} \begin{bmatrix} V_\alpha \\ V_\beta \end{bmatrix} \tag{3}$$

$$\begin{cases} V_d = V_\alpha \cos\theta^{'} + V_\beta \sin\theta^{'} \\ V_q = -V_\alpha \sin\theta^{'} + V_\beta \cos\theta^{'} \end{cases} \tag{4}$$

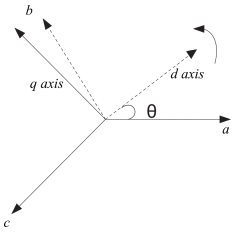

Figure 1: The Synchronous Rotating Reference Frame.

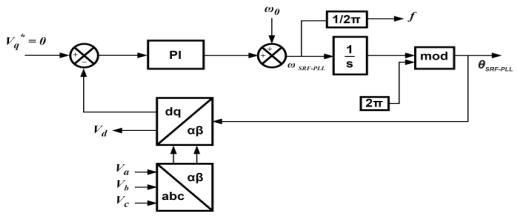

Figure 2: The SRF-PLL's scheme.

2.2. Tuning of PI Controller Gains

To find proportional and integral PI controller gains for SRF-PLL, the approximation $\sin(\Delta\theta) \approx \Delta\theta$ if $\Delta\theta \to 0$ is applied to Eq. (4), which leads to Eq. (5). The simplified model of the SRF-PLL becomes as seen in Fig. 3 and the closed-loop transfer function of it is in Eq. (6).

$$\begin{cases} V_d \approx V_m \\ V_q \approx -V_m(\theta - \theta^{'}) \end{cases} \tag{5}$$

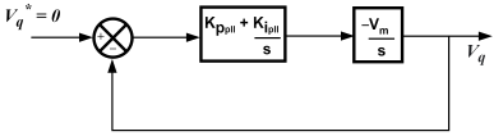

Figure 3: Simplified model of SRF-PLL.

$$G_{cl-srfpll}(s) = \frac{-V_m(K_{p-pll}s + K_{i-pll})}{s^2 - V_m K_{p-pll}s - V_m K_{i-pll}} \tag{6}$$

By matching Eq. (6)'s denominator to the second order system's standard form in Eq. (7) :

$$s^2 + 2\xi\omega_n s + \omega_n^2 \tag{7}$$

K_p and K_i are given by:

$$\begin{cases} K_{p-srfpll} = \frac{-2\xi\omega_n}{V_m} \\ K_{i-srfpll} = \frac{-\omega_n^2}{V_m} \end{cases} \tag{8}$$

3. Design of Fuzzy Logic Based SRF-PLL

Getting a faster response from the PI controller will lead to instability problems. Also, PI controllers are highly sensitive to varying parameters and sudden fluctuations, for example, in frequency or voltage during grid faults. Such controllers may not give the desired response. As mentioned in [5, 6] instead of regulating a precise mathematical model, fuzzy logic control is more suited for systems with unpredictability because it incorporates human-like understanding skills and physical characteristics of the system [4].

In this section the PI controller of the dq-PLL is substituted by the Fuzzy logic controller (FLC) as shown in Fig. 4. The design of the proposed FLC must follow to the structure shown in Fig. 5. The primary steps of the FLC can be categorized into three main stages: fuzzification, inference rules, and defuzzification [9].

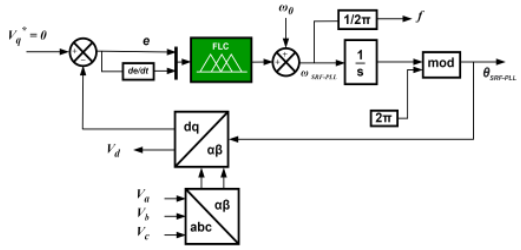

Figure 4: FLC based dq-PLL.

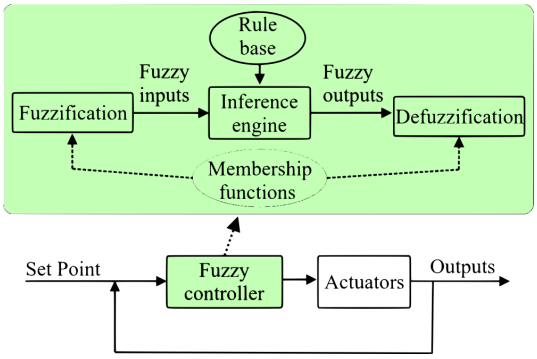

Figure 5: General structure of FLC.

The first input of this intelligent controller is the error ($E_{(k)}$), representing the difference between the reference value of the quadrature component of grid voltage (V_q^*) and its measured value (V_q), while the second input is the change in error ($CE_{(k)}$) is the derivative of $E_{(k)}$, as defined by Eq. (9).

$$\begin{cases} E_{(k)} = K_e(V_q^* - V_q) \\ CE_{(k)} = K_{ce}(E_{(k)} - E_{(k-1)})/T_{st} \end{cases} \quad (9)$$

The output of this controller is then multiplied by K_u before continuing its path in the loop to detect the phase angle.

With T_{st} is the sampling time and k_e, k_{ce}, and k_u are the scaling factors, these gains are very important in normalizing the input and output variables and for the performance and stability of the control system.

3.1. Fuzzification

In fuzzy logic systems, fuzzyification is the transformation of exact input values into fuzzy sets that represent input variables as linguistic variables and membership functions (MF) [5]. In this study, five linguistic variables are used to define the input and output variables as follow:

- NB : negative big
- NS : negative small
- Z : zero
- PS : positive small
- PB : positive big

MF of triangular shape are selected for each variable, as shown in Fig. 6.

3.2. Inference Engine and Rule Base

The Inference System is the fundamental component of FLC, since it is responsible for making decisions based on if-then fuzzy rules and fuzzy implication sub-blocks. The two most popular approaches used for this are Mamdani and Sugeno [10]. The fuzzy inference of this study is done with the Mamdani inference engine and the max-min implication technique, where the "AND" operator is represented by the MIN operation and the "OR" operator by the MAX operation. The 25 fuzzy rules that determine the FLC's output depending on its two inputs are indicated in Table 1. While Fig. 7 shows the control surface of the fuzzy rule base.

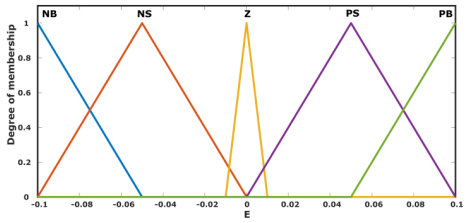

(a)

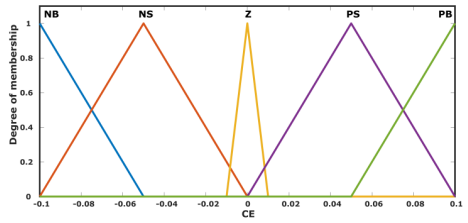

(b)

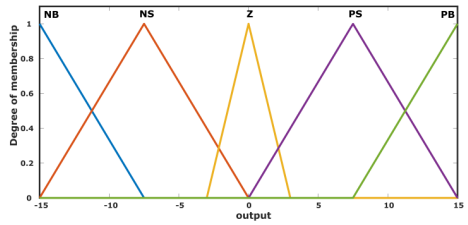

(c)

Figure 6: Membership functions for: (a) error, (b) change in error, and (c) FLC output.

Table 1
5x5 Fuzzy rules used in FLC based SRF-PLL.

		CE				
		NB	**NS**	**Z**	**PS**	**PB**
E	**NB**	NB	NB	NB	NS	Z
	NS	NB	NB	NS	Z	PS
	Z	NB	NS	Z	PS	PB
	PS	NS	Z	PS	PB	PB
	PB	Z	PS	PB	PB	PB

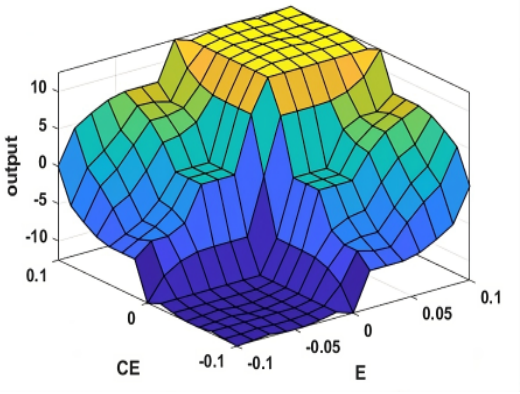

Figure 7: FLC rule surface.

3.3. Defuzzification

The fuzzy output result generated by the Mamdani inference engine in the form of MF is then transformed into a numerical value by employing defuzzification techniques such as the Center of Gravity (COG) and Mean of Maximum (MOM) methods [10]. In this research, COG is used during the defuzzification process. All previous design steps was implemented by Matlab fuzzy logic toolbox.

4. Simulation Results

To test the designed PLLs, both of them were placed in the control block of a predefined model of a three-phase grid-connected 2-level voltage source inverter (2L-VSI) as shown in Fig. 9 in order to evaluate the performance of each in such a system. Simulation tests were conducted in the Matlab/Simulink environment during normal grid conditions to evaluate their transient and steady-state responses. All parameters used in the test system are outlined in Table 2. The model used in this simulation is shown in Fig. 8.

Table 2
Performance characteristics of PLLs.

Inverter	V_{dc}	1025 V
	f_g	50 Hz
	V_{ac}	315 V
	f_{sw}	10 kHz
	P_{rated}	1 MW
LCL-Filter	Li	80.719 μH
	C_f	267.33 μF
	L_g	5.6852 μH
	R_d	0.0470 Ω
Transformers and transmission line	step-up transformer	315/31.5 kV
		1250 kVA
	R'	0.35 Ω/km
	X'	0.4 Ω/km
	B'	2.844 μS/km
	step-down transformer	220/31.5 kV
		30 kVA
PI controller for SRF-PLL	$K_{p\text{-}srfpll}$	-640
	$K_{i\text{-}srfpll}$	-204861.9

Here :
V_{dc}: the DC input voltage
V_{ac}: the AC output voltage
f_{sw}: the switching frequency
P_{rated}: the rated AC power
f_g: the grid frequency
L_i , L_g: inverter side and grid side inductance
C_f: filter capacitor
R_d: damding resistor
R', X', and B': per-unit-length resistance, reactance, and susceptance of transmission line

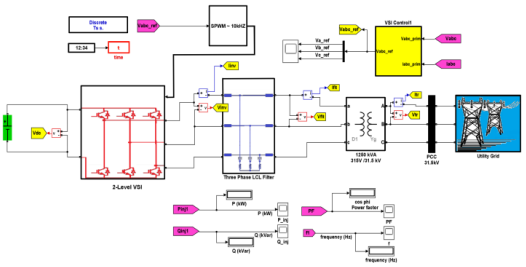

Figure 8: The 1 MW grid-connected inverter.

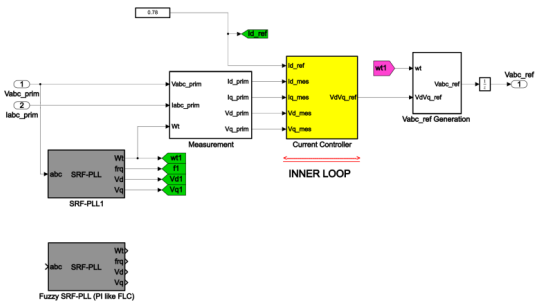

Figure 9: Implementation of PI and FLC based SRF-PLL in the Current controller of the grid-connected inverter.

4.1. Results for PI based SRF-PLL

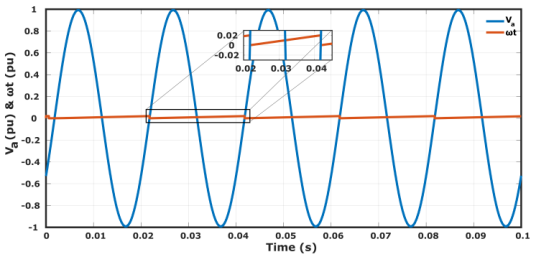

(a) Phase voltage and phase angle

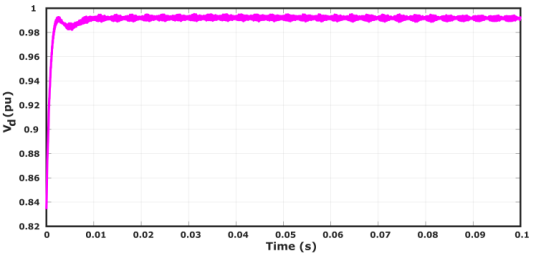

(b) Direct voltage component

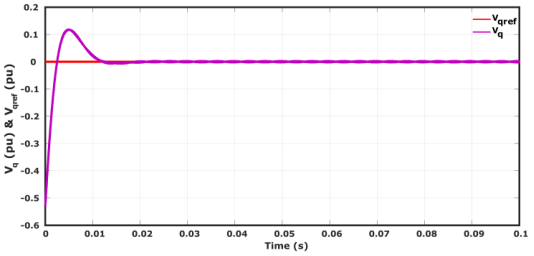

(c) Quadrature voltage component

Figure 10: Simulation results for PI based SRF-PLL in grid-connected inverter.

The plot in Fig. 10a demonstrate that the dq-PLL successfully detected the grid voltage phase accurately. Furthermore, the PI controller effectively regulated the quadrature component V_q to zero after a half cycle (0.01s), but with a noticeable overshoot as seen in Fig. 10c. On the other hand, as V_q is forced to zero, the direct component of the grid voltage V_d becomes constant and close to 1 per unit (pu) after a slight drop in the transient state, corresponding to the peak value of the grid voltage V_m, as mentioned in Eq. (5).

4.2. Results for FLC based SRF-PLL

Similarly to the previous simulation, PI based-PLL was replaced in the current controller of the 2L-VSI with the proposed FLC. The results are shown in Fig. 11.

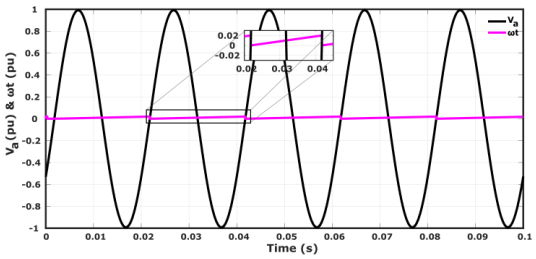

(a) Phase voltage and phase angle

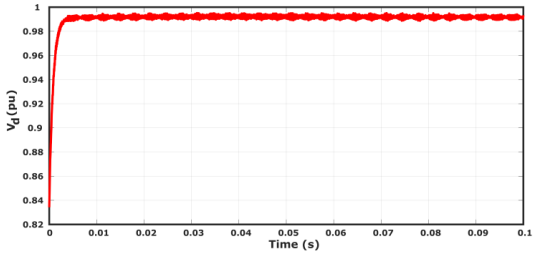

(b) Direct voltage component

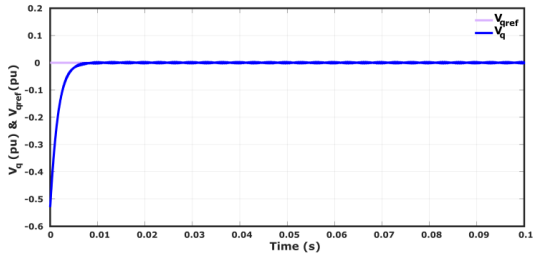

(c) Quadrature voltage component

Figure 11: Simulation results for FLC based SRF-PLL in grid-connected inverter.

Similar to the previous results, the FLC was able to effectively lock onto the grid phase. Notably, there is a marked improvement in the plot of V_q and V_{qref} in Fig. 11c compared to that of the PI controller. With the FLC, the quadrature voltage component was maintained at its reference without a significant overshoot and in less than half a cycle.

Additionally, in Fig. 11b V_d remains constant at 1 per unit without any transient disturbances, indicating that the FLC yields better results than the PI controller at this stage.

The frequency response for both PLLs was plotted in Fig. 12 to evaluate and compare their performance in this system. Table 3. presents the performance characteristics for each PLL.

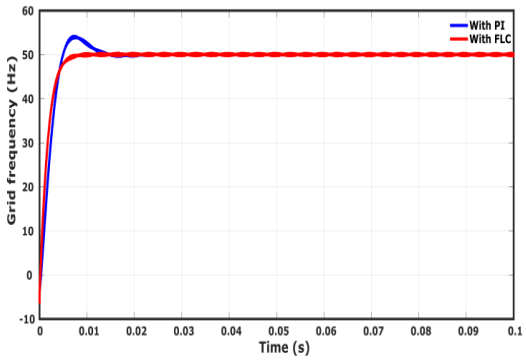

Figure 12: Frequency responses for PI based SRF-PLL and FLC based SRF-PLL

Table 3
Performance characteristics of PLLs.

	PI based SRF-PLL	FLC based SRF-PLL
Rise time (Tr)	3.5 ms	3.5 ms
Settling time (Ts)	9.8 ms	4.7 ms
Percentage overshoot (PO)	7.9062 %	0.3249 %
Peak value	54.1433 Hz	50.3659 Hz

By analyzing the frequency responses and performance characteristics of both PLLs, it can be confirmed that the proposed FLC controller outperformed the conventional PI controller not only in tracking the grid voltage phase and frequency but also in terms of the PLL performance within the VSI controller. The FLC-based PLL exhibited a low overshoot of 0.3249% and a short settling time of 4.7 ms. These results suggest that the FLC-based PLL could be a promising alternative to the conventional phase-locked loop.

5. Conclusion

In this research, the modeling and design of conventional and intelligent fuzzy logic controllers for synchronous reference frame phase-locked loops are presented. These PLLs were tested inside a 1 MW grid-connected VSI current controller predefined model. The different simulation results during normal grid conditions showed the effectiveness of both controllers in terms of detecting phase angle of grid voltage and reference tracking, but in terms of performance, the FLC-based SRF-PLL provided a better response compared to the PI-based SRF-PLL, reaching a short settling time with very low overshoot. These findings suggest that the FLC-based PLL could be a potential replacement for the traditional phase-locked loop, and much future work can be considered for this purpose.

Acknowledgments

The authors received no financial support for this research.

References

[1] M. P. Thakre, N. P. Matale, P. S. Borse, A survey based on pll and its synchronization techniques for interconnected system, in: International Conference on Artificial Intelligence and Smart Systems (ICAIS), IEEE, 2021, pp. 1011–1016. doi:https://doi.org/10.1109/ICAIS50930.2021.9395770.

[2] Z. Ali, N. Christofides, L. Hadjidemetriou, E. Kyriakides, Y. Yang, F. Blaabjerg, Three-phase phase-locked loop synchronization algorithms for grid-connected renewable energy systems: A review, Renewable and Sustainable Energy Reviews 90 (2018) 434–452. doi:https://doi.org/10.1016/J.RSER.2018.03.086.

[3] P. Tripathy, B. Misra, B. Nayak, A review on recent advanced three-phase plls for grid-integrated distributed power generation systems under adverse grid conditions, Springer Nature Singapore, 2023, pp. 17–29. doi:https://doi.org/10.1007/978-981-19-6605-7_2.

[4] Y. Wang, J. Song, F. Cao, Study on a novel fuzzy pll and its application, in: International Workshop on Intelligent Systems and Applications, IEEE, 2009, pp. 1–3. doi:https://doi.org/10.1109/IWISA.2009.5073130.

[5] M. Sibanyoni, S. D. Chowdhury, L. Ngoma, Single Phase Inverter Fuzzy Logic Phase Locked Loop, John Wiley and Sons, Ltd, 2021, pp. 91–120. doi:https://doi.org/10.1002/9781119710905.ch4.

[6] A. R. Gangula, S. Lakshmanan, B. S. Rajpurohoit, C. Prakash, T. Chandrasekaran, Design of fuzzy based pll for grid connected inverter under non-ideal grid conditions, in: IEEE IAS Global Conference on Renewable Energy and Hydrogen Technologies (GlobConHT), IEEE, 2023, pp. 1–6. doi:https://doi.org/10.1109/GlobConHT56829.2023.10087408.

[7] K. Fuad, Grid-voltage Synchronization Algorithms Based on Phase-locked Loop and Frequency-locked Loop for Power Converters, Thesis, 2014. doi:http://dx.doi.org/10.13140/RG.2.2.25940.12166.

[8] N. Mennai, Y. Soufi, A. Medoued, A. Faleh, Grid synchronization techniques analysis of dg systems under grid fault conditions, in: 19th International Multi-Conference on Systems, Signals and Devices

(SSD), IEEE, 2022, pp. 917–922. doi:https://doi.org/10.1109/SSD54932.2022.9955866.

[9] N. Ikken, A. Bouknadel, H. El Omari, H. El Omari, Design and implementation of intelligent pi-fuzzy logic control for grid connected inverters, in: International Renewable and Sustainable Energy Conference (IRSEC), IEEE, 2016, pp. 1111–1117. doi:https://doi.org/10.1109/IRSEC.2016.7984022.

[10] A. Guidara, Policy decision modeling with Fuzzy Logic: Theoretical and computational aspects, volume 405, Springer Nature, 2020. doi:https://doi.org/10.1007/978-3-030-62628-0.